Compositional variation in tourmaline from tourmalinite and quartz segregations at Pernštejn near Nedvědice (Svratka Unit, western Moravia, Czech Republic)

Variace v chemickém složení turmalínu z turmalinitu a křemenných segregací od Pernštejna u Nedvědice (svratecké krystalinikum) (Czech summary)

(2 text-figs.)

STANISLAV HOUZAR[1] - MILAN NOVÁK[1] - JULIE B. SELWAY[2]

[1]*Department of Mineralogy and Petrography, Moravian Museum, Zelný trh 6, 659 37 Brno, Czech Republic*
[2]*Department of Geological Sciences, University of Manitoba, Winnipeg R3T 2N2, Canada*

The Pernštejn tourmalinite is situated in the southern part of the Svratka Unit near the border with Moldanubicum. It underwent a retrogressive low-to-medium grade regional metamorphism which produced quartz segregations within the tourmalinite. Fine-grained tourmalinite dominantly consists of quartz and tourmaline (dravite-schorl). The tourmaline is elongated, euhedral to subhedral grains are typically < 0.5 mm in size. Tourmaline (dravite-schorl) from quartz segregations forms euhedral grains, from 0.5 to 10 mm in size, locally associated with kyanite, andalusite, muscovite, apatite and accessory rutile. There is only a negligible difference between tourmaline from tourmalinite and quartz segregations. Tourmaline of both paragenetic types is characterized by moderate to high vacancies in the X-site, up to 45 at.%, and moderate to high F contents varying from 0.32 to 0.56 apfu. It also exhibits Fe/Mg ratios and Al contents typical for tourmaline in metapelites and metapsammites with an Al-saturating phase (e.g., kyanite, andalusite).
Formation of the quartz segregations with coarse-grained tourmaline and kyanite began during a retrogressive kyanite grade metamorphic event at P > 3-4 kbar and T > 400-500 °C through the kyanite-andalusite transition to the andalusite grade. The presence of tourmaline as the only ferro-magnesium mineral and the presence of Si-, Al- and Ti-saturating phases, i.e., quartz, kyanite/andalusite and rutile, respectively, buffered these elements during the mobilization process which produced the quartz segregations.

Key words: dravite, schorl, electron microprobe analyses, tourmalinite, quartz segregations, Svratka Unit

Introduction

Tourmaline is a highly refractory mineral stable over a very wide range of PTX conditions (e.g., Werding - Schreyer 1996). In regional metamorphic rocks, tourmaline crystallizes due to a reaction of B-rich fluids with ferro-magnesian minerals (e.g., biotite, cordierite, staurolite). These B-rich fluids infiltrate the host rock from an external source or were produced internally during regional metamorphism from B-bearing minerals (e.g., clay minerals, micas).

Tourmaline-rich quartzite and tourmalinites are rare but relatively widespread members in volcanosedimentary complexes (Slack 1996). The tourmalinites from Pernštejn underwent low to medium grade regional metamorphism. A retrogressive stage produced the associated quartz-rich segregations. The compositional variation in tourmaline from tourmalinite and quartz segregations at locality Pernštejn near Nedvědice is discussed in this paper.

Geological setting

The Pernštejn locality is situated in the southern part of the Svratka Unit near the border with the Moldanubicum (Fig. 1). The area consists of dominant medium- to coarse-grained lepidoblastic schists, locally with accessory kyanite, garnet, staurolite, sillimanite and tourmaline. The mica schists are interlayered with fine-grained two-mica paragneisses, locally migmatized, rare marbles, Fe-skarns, amphibolites and serpentinites. They also contain numerous elongated bodies of muscovite and two-mica orthogneisses which are locally tourmaline-bearing (Němec 1979, Pertoldová et al. 1987, Novák et al. 1997). Typically, tourmaline is a relatively abundant accessory to minor phase in most rocks within the southern part of the Svratka Unit.

Metamorphism in the Svratka Unit has been studied by several authors (e.g., Frejvald 1965, Němec 1968), however, calculated P-T data is scarce and controversial (Pertoldová et al. 1987, Štoudová et al. 1997). The rock sequence underwent a dominant regional kyanite-staurolite metamorphic event. It was only locally overprinted by a later metamorphic event characterized by higher T and/or lower P conditions particularly along its SW border with the Strážek Moldanubicum. The metapelites contain the following mineral assemblages: garnet + staurolite + kyanite and garnet + biotite + sillimanite; the latter assemblage may be an overprint. Garnet-biotite thermometer calculations in metapelites indicate T = 550-620 °C at P = 8-11 kbar for the northeastern part of the Svratka Unit (Štoudová et al. 1997); however, Pertoldová et al. (1987) found T = 600-725 °C at P about 5 kbar for skarn and associated metapelite close to the tourmalinite locality. A migmatization is locally developed, and seems to be somehow related to the younger metamorphic event (Němec 1968). The sequence of metamorphic events and their regional distribution within the Svratka Unit are not well understood.

Occurrence

Tourmalinite is hosted by underlying mica schist and overlying paragneiss (Páša et al. 1994). Mica schist is strongly foliated, medium- to coarse-grained and consists of dominant elongated quartz grains, flakes of muscovite, minor garnet, biotite and rare plagioclase.

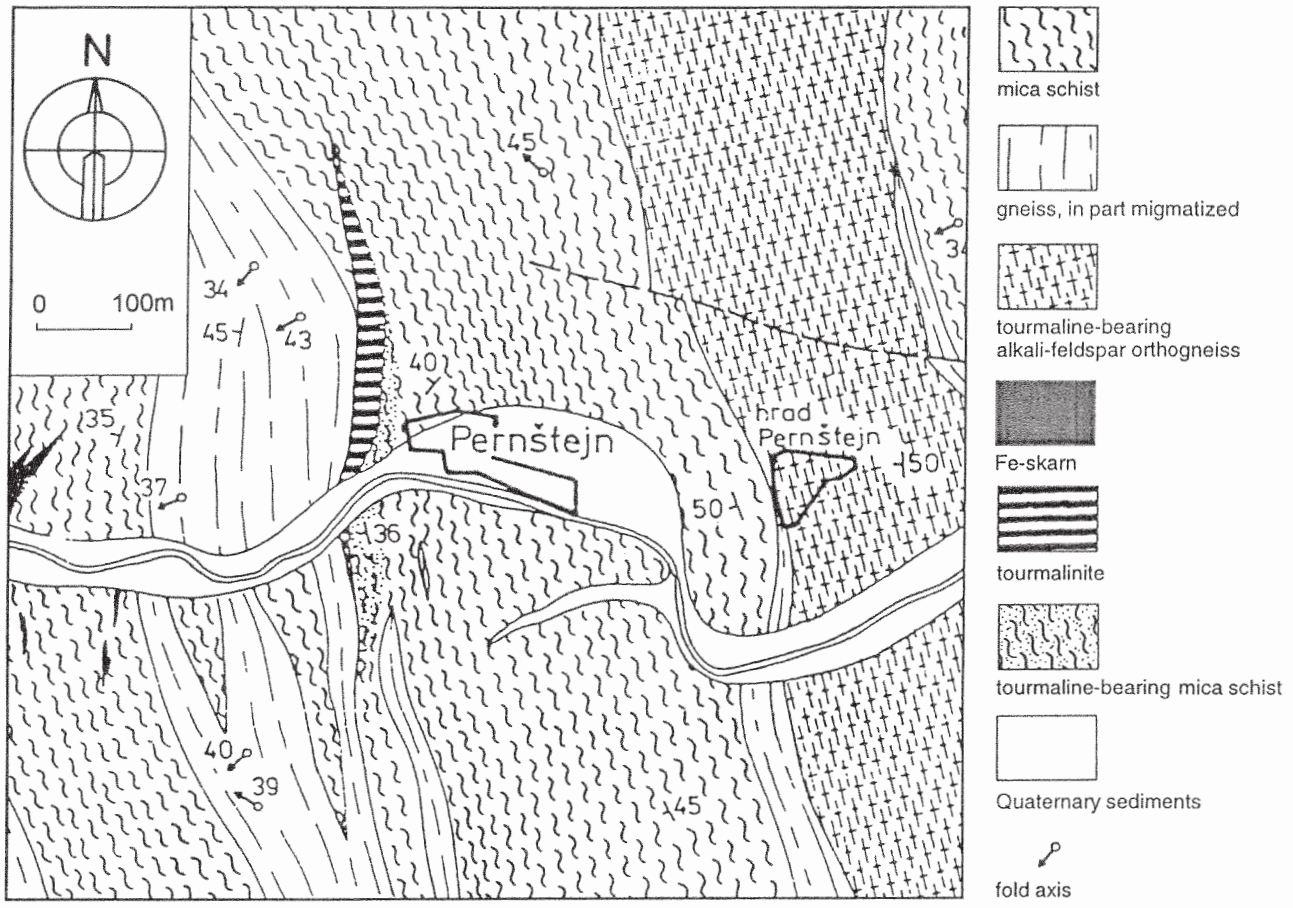

Fig. 1. Schematic geological map of the Pernštejn area (modified from Pertoldová et al. 1987)

Accessory minerals in the mica schist include tourmaline, kyanite, sillimanite, rutile, apatite and zircon. Locally migmatized, medium-grained two-mica gneiss consists of quartz, plagioclase, muscovite, biotite, accessory apatite and zircon.

Tourmalinite forms conformable folded layers and boudins, up to 1 m thick and several metres long. Numerous fragments of tourmaline-rich rocks found in southern part of the Svratka Unit (at localities Litava, Pernštejn, Kovářova, Ujčov, Lesoňovice) indicate that they form a N-S trending discontinuous belt, up to 15 km long (Houzar et al. 1997). Due to relatively strong polyphase metamorphism and tectonic reworking, premetamorphic formation of tourmaline-rich rocks is not easy to explain. Based on the associated rock sequence, lithology of tourmaline-bearing rocks and the chemical composition of tourmaline, Houzar et al. (1997) suggested a submarine-hydrothermal replacement of clastic sediments by B-rich fluids (Slack 1996) as a likely origin. However, the source of the B-rich fluids is unknown.

Quartz segregations locally with abundant tourmaline or kyanite/andalusite form irregular lenses and discordant veins commonly enclosed in tourmalinites. The quartz segregations are up to 50 cm thick and several metres long, but small veins, up to several cm's thick, are typical. Contact with the host rock is commonly sharp with rare mobilized tourmaline grains located along the contact. Segregations also exhibit folding and preferential orientation of kyanite and muscovite.

Petrography of tourmaline-bearing rocks

Tourmalinite

Fine-grained tourmalinites to tourmaline-rich quartzites dominantly consist of quartz and tourmaline, which may locally predominate over quartz; tourmaline contents vary from 15 to 30 vol.% in volumetrically dominant rock. Tourmaline forms elongated, euhedral to subhedral grains, typically < 0.5 mm, containing small inclusions of rutile and locally also apatite. They are concentrated in narrow layers and exhibit preferred orientation. Tourmaline is homogeneous or slightly zoned in thin section with the pleochroism: O = dark greenish brown, E = pale yellowish brown. Muscovite and kyanite are usually minor to accessory minerals, but may locally display elevated volume percentages. Accessory minerals also include rutile, garnet, apatite and zircon.

Quartz segregations

Three distinct mineral assemblages were observed in ductile quartz segregations: (i) quartz dominant large veins with negligible amount of other minerals (muscovite, tour-

Table 1. Representative compositions of tourmaline from Pernštejn

	1/r	1/c	2/r	2/c	3/r	3/c	4/r	4/c
P_2O_5	0.00	0.00	0.00	0.01	0.05	0.00	0.00	0.01
SiO_2	35.90	36.60	35.80	35.80	36.20	35.70	35.70	36.20
B_2O_3*	10.45	10.47	10.52	10.46	10.49	10.47	10.43	10.50
TiO_2	0.51	0.54	0.54	0.36	0.31	0.25	0.65	0.57
Al_2O_3	33.10	32.30	33.70	33.70	33.00	33.70	32.10	31.90
MgO	4.94	5.05	4.90	4.01	4.65	4.86	5.65	6.03
CaO	0.26	0.35	0.26	0.36	0.64	0.34	0.69	0.92
MnO	0.00	0.04	0.00	0.00	0.01	0.00	0.00	0.02
FeO**	8.06	8.17	8.17	9.34	8.92	8.31	8.37	8.01
ZnO	0.06	0.00	0.00	0.02	0.00	0.03	0.00	0.00
Na_2O	1.81	1.49	1.87	1.47	1.54	1.75	1.83	1.69
K_2O	0.06	0.35	0.07	0.10	0.06	0.05	0.04	0.02
F	0.98	0.84	0.92	0.75	0.84	0.61	0.92	1.07
H_2O*	3.14	3.21	3.19	3.25	3.22	3.32	3.16	3.12
O=F	-0.41	-0.35	-0.39	-0.32	-0.35	-0.26	-0.39	-0.45
TOTAL	98.86	99.06	99.55	99.31	99.58	99.14	99.16	99.60
T-Si	5.97	6.08	5.92	5.95	6.00	5.92	5.95	5.99
P	0.00	0.00	0.00	0.00	0.01	0.00	0.00	0.00
Al	0.03	-	0.08	0.05	-	0.08	0.05	0.01
Z-Al	6.00	6.00	6.00	6.00	6.00	6.00	6.00	6.00
Y-Ti	0.06	0.07	0.07	0.05	0.04	0.03	0.08	0.07
Al	0.46	0.32	0.48	0.55	0.44	0.51	0.25	0.21
Mg	1.23	1.25	1.21	0.99	1.15	1.20	1.40	1.49
Mn^{2+}	0.00	0.01	0.00	0.00	0.00	0.00	0.00	0.00
Fe^{2+}	1.12	1.13	1.13	1.30	1.24	1.15	1.17	1.11
Zn	0.01	0.00	0.00	0.00	0.00	0.00	0.00	0.00
Σ Y	2.88	2.78	2.89	2.89	2.87	2.89	2.90	2.88
X-Ca	0.05	0.06	0.05	0.06	0.11	0.06	0.12	0.16
Na	0.58	0.48	0.60	0.47	0.50	0.56	0.59	0.54
K	0.01	0.07	0.02	0.02	0.01	0.01	0.01	0.00
Σ X	0.64	0.61	0.67	0.55	0.62	0.63	0.72	0.70
F^-	0.52	0.44	0.48	0.39	0.44	0.32	0.49	0.56
OH^+	3.48	3.56	3.52	3.61	3.56	3.68	3.51	3.44

* - calculated from stoichiometry; ** total Fe as FeO, 1-2 - tourmalinite; 3-4 - quartz segregation; r - rim; c - core

maline); (ii) small veins with abundant tourmaline and minor rutile, apatite, muscovite; (iii) small veins with abundant kyanite/andalusite + muscovite + rare tourmaline and rutile. The latter assemblages may vary even within an individual quartz segregation. Quartz dominant veins are evidently the most widespread and form the largest veins, whereas abundant schorl and/or kyanite/andalusite are evidently concentrated into small satellite veins, up to 5 cm thick. Small veins exhibit increasing degree of folding relative to the large quartz dominant veins. Tourmaline forms euhedral equidimensional grains or needles, 0.5 to 10 mm in size. Tourmaline is commonly homogeneous or slightly concentrically zoned in thin section with the pleochroism: O = dark brown, E = pale yellowish brown.

Chemical composition

Electron microprobe analyses were carried out in the WDS (wavelength-dispersive) mode on a Cameca SX-50 instrument, Department of Geological Sciences, University of Manitoba, Winnipeg, with a beam diameter 1 μm, accelerating potential 15 kV. A beam current 20 nA was used for Si, Al, Fe, Mg, Ca, and Na, the current of 40 nA for P, Ti, Mn, Zn, F and K; a counting time for all elements is 20 seconds. The following standards were used for Kα X-ray lines: Si, Ca-diopside; Al-kyanite; Fe-fayalite; Ti-rutile; Mg-pyrope; Mn-spessartine; Na-albite; K-orthoclase; P-apatite; F-fluor-riebeckite and Zn-gahnite. Data were reduced using the PAP routine (Pouchou - Pichoir 1985).

Tourmaline has the general formula $XY_3Z_6(BO_3)_3T_6O_{18}(O,OH)_3(OH,F)_1$, where X = Na, Ca, vacancy and K; Y = Li, Fe^{2+}, Mg, Mn, Zn, Al, Cr^{3+}, V^{3+}, Fe^{3+}, Ti; Z = Al, Mg, Fe^{3+}, Cr^{3+}, V^{3+}; and T = Si, Al. The structural formulae were calculated on the basis of 31 anions assuming OH + F = 4, and B = 3 atoms per formula units (apfu). These recalculated compositions have oxide totals of approximately 100 wt.% and the Y-site totals are close to the ideal value of 3.0 apfu.

The tourmaline compositions from tourmalinite and quartz segregations form a tight cluster in the Al-Fe(tot)-Mg diagram (Houzar et al. 1997) and are homogeneous in BSE images. Dravite predominates over schorl in most analyses (Table 1, Fig. 2a).

T-site and Z-site

The T-site is usually fully occupied by Si in both paragenetic types of tourmaline. Only some compositions indicate that minor amounts of Al, up to 0.14 apfu, may enter

T-site. All compositions display Al > 6 apfu. Therefore, the Z-site is very likely fully occupied by Al for both paragenetic types disregarding a possible Al-Mg disorder (Grice - Ercit 1993).

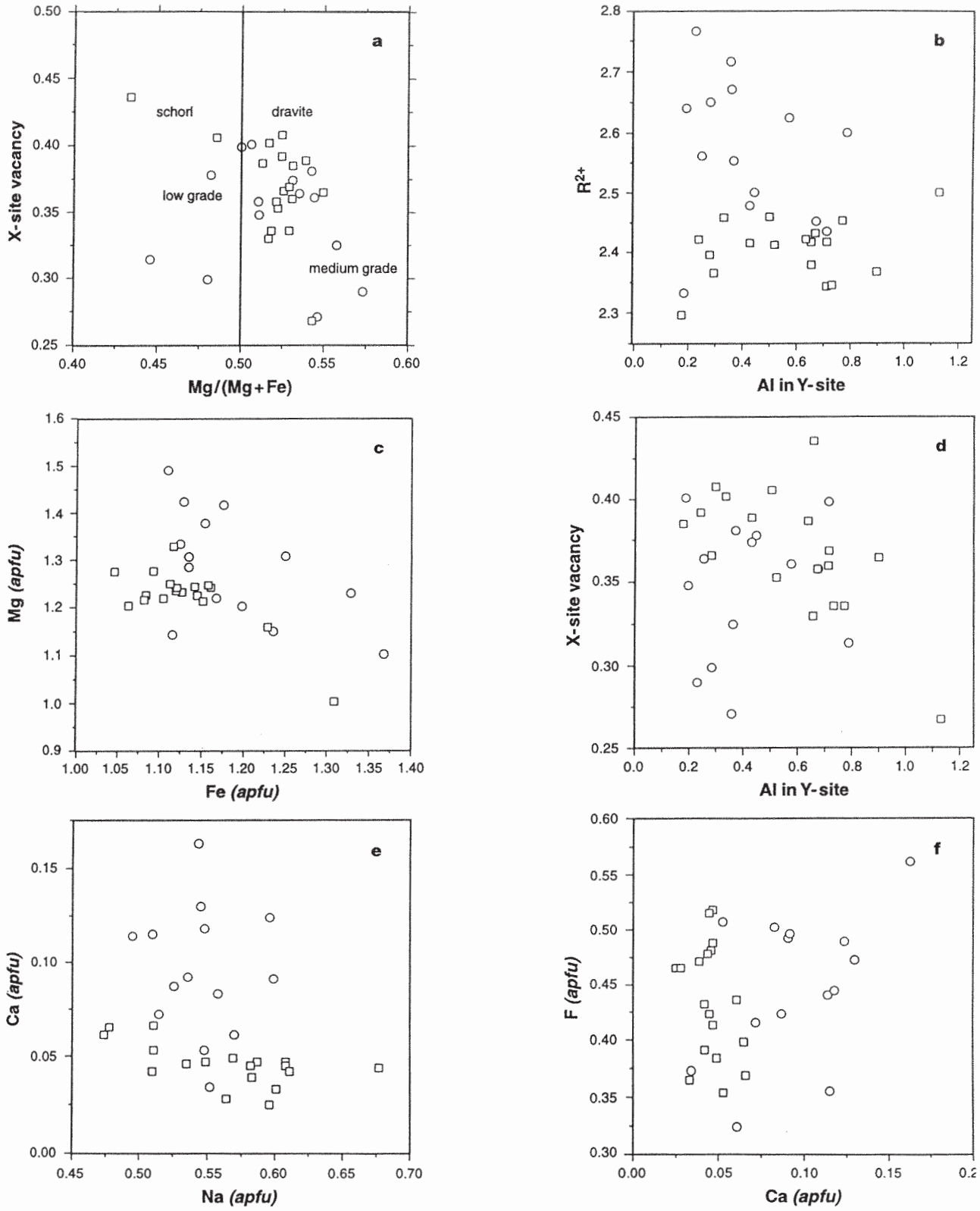

Fig. 2. Composition of tourmaline from tourmalinite and quartz segregations given in atoms per formula unit (apfu)
squares - tourmaline from tourmalinite; *circles* - tourmaline from quartz segregations; a) X-site vacancy versus Mg/(Mg + Fe) ratio; low grade and medium grade fields of tourmaline compositions taken from Henry - Dutrow (1996); b) R^{2+} versus Al at Y-site, R^{2+} = Fe + Mg + Mn + Zn + Ca; c) Mg versus Fe; d) X-site vacancy versus Al at Y-site; e) Ca versus Na; f) F versus Ca

Y-site

The Al contents at the Y-site range from 0.18 to 0.80 apfu and 0.18 to 1.12 apfu in tourmaline from quartz segregations and from tourmalinite, respectively (Fig. 2b). The Ti content ranges from 0.03 to 0.08 apfu and it is slightly larger for tourmaline from quartz segregations than that from tourmalinite. It also exhibits slightly elevated Mg and decreased Fe contents (Fig. 2c). There is a negative correlation between Mg and Fe in tourmaline from both paragenetic types (Fig. 2c). The Mn and Zn contents are commonly near or below the detection limit (Table 1).

X-site

Tourmaline in both paragenetic types is characterized by moderate to high vacancies in the X-site, up to 45 at.%, which are slightly higher in tourmaline from tourmalinite (Fig. 2d). Elevated Ca, up to 0.16 apfu, was found particularly in tourmaline from quartz segregations, whereas tourmaline from tourmalinite exhibits low Ca (Fig. 2e). Relatively high K, up to 0.07 apfu, was sporadically determined in the core of a dravite-schorl crystal from tourmalinite (Table 1).

Monovalent anions

Tourmaline shows moderate to high F contents, varying from 0.32 to 0.56 apfu. It is very similar in both paragenetic types, but has a slightly wider range for tourmaline from quartz segregations. There is a positive correlation between F and Ca in tourmaline from quartz segregations (Fig. 2f).

Discussion

The chemical compositions of tourmaline from both paragenetic types are very similar and differences may be summarized as follows: slightly elevated Ca, Mg and Ti contents in tourmaline from quartz segregations whereas tourmaline from tourmalinite is slightly Al enriched. Low Mn and Zn contents and variable F contents are similar in both paragenetic types. The negligible differences in tourmaline composition and absence of B_2O_3 and H_2O determinations from both paragenetic types make it difficult to predict reliable substitutions; however, homovalent substitution Fe-Mg in tourmaline from tourmalinite and quartz segregations is very likely (Fig. 2c).

Tourmaline from tourmalinite and quartz segregations exhibits Fe/Mg ratios and Al contents typical for tourmaline from metapelites and metapsammites coexisting with an Al-saturating phase (e.g., kyanite, andalusite) (Henry - Guidotti 1985). The F contents and X-site vacancies are slightly higher than those found in low to medium grade metapelites and quartzites (Henry - Dutrow 1996). Elevated F contents are typical for all tourmaline examined from the Svratka Unit (Němec 1968, Povondra 1981, Povondra - Novák 1986, Novák et al. 1997). Combination of relatively high vacancies at the X-site and high F contents observed in both paragenetic types is unusual for tourmaline (Robert et al. 1997) and contrasts with extremely low X-site vacancies in tourmaline from related rocks at locality Nedvědice (Novák et al. 1997).

The textural relationships and mineral assemblages of tourmaline-bearing rocks indicate a polymetamorphic origin comparable to their host rocks under P-T conditions discussed above. The regional metamorphism of tourmalinites was followed by the formation of quartz segregations. Textural relations of Al_2SiO_5 minerals in thin quartz segregations show kyanite-andalusite equilibrium in some thin sections but evidence of replacement of kyanite by late andalusite is seen in most thin sections. Absence of sillimanite, diaspore and/or pyrophyllite is typical for all studied samples. Based on the P-T diagram (Perkins et al. 1979), these observations suggest formation of the segregations began during a regrogressive phase at kyanite metamorphic grade at $P > 3$-4 kbar and $T > 400$-500 °C through the kyanite-andalusite transition to the andalusite grade.

The abundance of quartz, tourmaline, kyanite/andalusite, rutile, apatite and muscovite in quartz segregations documents the mobility of Si, Ti, Al, B, Fe, Mg, Ca, Na, K, P, H_2O and F. However, large quartz veins very likely formed during a lower-temperature process than the small, more folded tourmaline- or kyanite/andalusite-rich veins. General variability in mineral composition of quartz segregations from those with abundant tourmaline or kyanite to those with dominant quartz may be explained by a decreasing temperature of crystallization. There is only a negligible difference between the chemical composition of fine-grained tourmaline in tourmalinite and coarse-grained tourmaline from the quartz segregations found. The presence of tourmaline as the only ferro-magnesium mineral and the Si-, Al- and Ti-saturating phases, i.e., quartz, kyanite/andalusite and rutile, respectively, buffered these elements. The mobilization process producing quartz segregations with coarse-grained tourmaline almost replicated the composition of the fine-grained tourmaline. Elevated Ca in tourmaline from segregations and associated apatite reflect increased activity of Ca. Plagioclase from host rocks may be the Ca source. Slightly depressed Al contents in the tourmaline from segregations may be controlled by the associated Al-saturating phases, kyanite/andalusite and/or the lower temperature of crystallization.

Acknowledgements. We authors are indebted to J. Zimák for helpful comments which significantly improved the paper. The work was funded by the Grant Agency of the Academy of Sciences of Czech Republic, Grant No. A3408601 for SH and MN. It was also supported by a University of Manitoba Fellowship to JBS and by Natural Science and Engeneering Research Council of Canada Operating, Infrastructure and Major Equipment Grant to F. C. Hawthorne.

Submitted November 15, 1997

References

Frejvald, M. (1965): Styk svorové zóny a svratecké klenby jihovýchodně od Víru na Moravě. - Sbor. geol. Věd, Geol., 7, 37-58.

Grice, J. D. - Ercit, T. S. (1993): Ordering of Fe and Mg in the tourmaline crystal structure: the correct formula. - Neu. Jb. Mineral., Abh., 165, 245-26.

Henry, D. J. - Dutrow, B. (1992): Tourmaline in a low grade clastic metasedimentary rock: an example of the petrogenetic potential of tourmaline. - Contr. Mineral. Petrology, 112, 203-218.

- (1996): Metamorphic tourmaline and its petrologic applications. *In: E. S. Grew - L. M. Anovitz* (eds.): Rev. Mineral., 33 (Boron Mineralogy, Petrology and Geochemistry), 503-557.

Henry, D. J. - Guidotti, V. Ch. (1985): Tourmaline as a petrogenetic indicator mineral: an example from the staurolite-grade metapelites of NW Maine. - Amer. Mineralogist, 70, 1-15.

Houzar, S. - Novák, M. - Selway, J. B. (1997): Pernštejn near Nedvědice. Metamorphosed tourmalinites in mica schists. *In: M. Novák - J. B. Selway* (eds.): Field Trip Guidebook, International Symposium Tourmaline 1997, June 1997, 71-76. Nové Město na Moravě.

Němec, D. (1968): Die Metamorphose des NE-Randes des Kernes der Böhmischen Masse. - Verh. Geol. Bundesanst., 1-2, 189-203.

- (1979): Zinnbringende Orthogneise im Süden der Antiklinale von Svratka (nordwestlich Brno) und ihre Erzmineralisierung. - Z. geol. Wiss., 7, 12, 1437-1447.

Novák, M. - Selway, J. B. - Houzar, S. - Uher, P. (1997): Nedvědice. Leucocratic orthogneiss, mica schists layers and fluorite-dominant layer with abundant tourmaline. *In: M. Novák - J. B. Selway* (eds.): Field Trip Guidebook, International Symposium Tourmaline 1997, June 1997, 39-46. Nové Město na Moravě.

Páša, J. - Hranáč, P. et al. (1994): Turmalínové horniny - MS, závěrečná zpráva úkolu 29 90 2301, GMS a.s. Praha, Jihlava.

Perkins, D. III. - Essene, E. J. - Westrum, E. F. jr. - Wall, V. J. (1979): New thermodynamic data for diaspore and their application to the system Al_2O_3-SiO_2-H_2O. - Amer. Mineralogist, 64, 1080-1090.

Pertoldová, J. - Pudilová, M. - Pertold, Z. (1987): Podmínky vzniku skarnu na lokalitě Pernštejn (svratecké krystalinikum). - Sbor.: Nové trendy a poznatky v československé ložiskové geologii, 43-61. Přírodověd. fak. Univ. Karlovy. Praha.

Pouchou, J. L. - Pichoir, F. (1985): "PAP" procedure for improved quantitative microanalysis. - Microbeam Anal., 20, 104-105.

Povondra, P. (1981): The crystal chemistry of tourmalines of the schorl-dravite series. - Acta Univ. Carol., Geol., 223-264.

Povondra, P. - Novák M. (1986): Tourmalines in metamorphosed carbonate rocks from western Moravia, Czechoslovakia. - Neu. Jb. Mineral., Mh., 1986, 273-282.

Robert, J. L. - Groudant, J. P. - Linnen, R. L. - Roeuer, O. - Benoist, P. (1997): Crystal-chemical relationships between OH, F and Na in tourmalines. - Abstracts, International Symposium Tourmaline, June 1997, 84-85. Nové Město na Moravě.

Slack, J. F. (1996): Tourmaline Associations with Hydrothermal Ore Deposits. *In: E. S. Grew - L. M. Anovitz* (eds.): Rev. Mineral., Vol. 33 (Boron Mineralogy, Petrology and Geochemistry), 117-163.

Štoudová, S. - Schulmann, K. - Konopásek, J. (1997): Kontrastní PT a strukturní vývoj vírské granulitové megabudiny a okolních metapelitů: Poličské krystalinikum, východní okraj Českého masívu. - Sbor. II. semináře České tektonické skupiny, 69-70, Ostrava.

Werding, G. - Schreyer, W. (1996): Experimental Studies on Borosilicates and Selected Borates. *In: E. S. Grew - L. M. Anovitz* (eds.): Rev. Mineral., 33, 117-163. (Boron Mineralogy, Petrology and Geochemistry).

Variace v chemickém složení turmalínu z turmalinitu a křemenných segregací od Pernštejna u Nedvědice (svratecké krystalinikum)

Turmalinity u Pernštejna, v j. části svrateckého krystalinika, jsou tvořeny turmalínem a křemenem, lokálně i kyanitem, muskovitem a rutilem. V retrográdní fázi MP-HT metamorfózy v nich vznikly křemenem bohaté segregace s kyanitem, andalusitem, muskovitem, apatitem a turmalínem. Turmalíny z obou asociací mají téměř totožné složení, skoryl-dravit, vyznačují se průměrnými až vyššími vakancemi v X-pozici a průměrnými a vyššími obsahy F. Chemické složení odpovídá turmalínům metapelitů a metapsamitů s Al-bohatými minerály (např. kyanit, andalusit). Retrográdní metamorfóza spojená se vznikem křemenných segregací za podmínek P > 300-400 MPa a T > 400-500 °C, pravděpodobně blízko hranice kyanit-andalusit, neměla vliv na podstatnější změnu složení turmalínu.

Chemistry and origin of povondraite-bearing rocks from Alto Chapare, Cochabamba, Bolivia

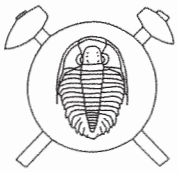

Chemismus a původ hornin s povondraitem z Alto Chapare, Cochabamba, Bolívie (Czech Summary)

(6 text-figs.)

VLADIMÍR ŽÁČEK[1] - ALFREDO PETROV[2] - JAROSLAV HYRŠL[3]

[1]*Czech Geological Survey, Klárov 3, 118 21 Praha 1, Czech Republic*
[2]*P.O. BOX 1728, Cochabamba, Bolivia*
[3]*Heverova 222, 28 000, Kolín 4, Czech Republic*

Povondraite and schorl-dravite occur in an ancient, probably Cambrian, metaevaporite known as the Locotal Breccia in Alto Chapare, Cochabamba Department, central Bolivian Andes. They originated, together with a variety of silicate minerals as reaction crust between dikes of highly alkaline volcanites, and B-rich evaporite. Chemical composition of the protolith (mainly various concentrations of alkalis) and local oxygen activity probably played decisive role in the formation either of povondraite or schorl-dravite. There are relatively small differences in SiO_2 (42-50 wt.%) and Al_2O_3 (12.2-15.5 wt.%), all rocks are relatively rich in TiO_2 (0.85-3.00 wt.%) and poor in CaO (0.0X-0.34 wt.%). The rocks rich in povondraite have extremely high concentrations of K_2O (10-12 wt.%), low Na_2O (0.4-0.7 wt.%), very low CaO (0.0X-0.13 wt.%) and increased Cr_2O_3 (about 0.1 wt.%), whereas the rock rich in dravite is slightly richer in CaO (0.34 wt.%) and the concentrations of both Na_2O and K_2O are about 4 wt.%. The concentrations of MgO (2.6-9.0 wt.%) and FeO^{tot} (5.4-13.0 wt. %) are variable and independent on given type of tourmaline.

Povondraite displays both continuous and oscillatory zoning patterns and chemical variability ranging in (wt.%): $Fe_2O_3^{tot}$ = 29.5-42.4, Al_2O_3 = 2.39-10.90, TiO_2 = 0.38-3.48, Na_2O = 1.45-2.29, K_2O = 1.15-2.35, and strongly variable Cr_2O_3 (0.0-1.36). Povondraite compositions differ from the ideal end-member formula $NaFe_3^{3+}Fe_6^{3+}(BO_3)_3(Si_6O_{18})(O,OH)_4$ by a constant presence of MgO ranging from 6 to 8 wt.% and potassium X-site occupancy of 25-48 at.%. The highest TiO_2 and K_2O concentrations recorded (3.48 and 2.35 wt.%, respectively) represent the upper concentration levels of these oxides in tourmaline. Successive crystallization of povondraite (1) - intermediate dravite-povondraite (2) and dravite-schorl (3) gives evidence for decreasing oxygen activity during tourmaline crystallization.

Key words: tourmaline, povondraite, schorl-dravite, electron microprobe composition, metaevaporite, Locotal Breccia, Bolivia

Introduction

Povondraite, a new member of the tourmaline group was desribed originally as *"ferridravite"* by Dunn - Walenta (1979) and redefined and renamed by Grice et al. (1993) in honour of Czech mineralogist and well-known tourmaline specialist Dr. P. Povondra (Charles University, Prague). *Povondraite* occurs with many additional minerals in a highly unusual rock called the Locotal Breccia, which represents brecciated metamorphosed evaporite caprock. Locotal Breccia outcrops sporadically within a roughly 50 km^2 area of highly disected rainforest topography in the Alto Chapare region, Cochabamba Department, Bolivia, in the steep eastern foothills of the Andes at an altitude between 400 to 2000 metres (Franz et al. 1979, Petrov 1994).

This paper brings new data on mineral assemblages, compositons and origin of povondraite-bearing rocks from Alto Chapare, Bolivia.

Geology and mineralogy of the Locotal Breccia

The Locotal Breccia most probably represents ancient slightly metamorphosed saltdome caprock (Petrov et al. 1997). This Cambrian (or Late Proterozoic) unit is the oldest rock in the central Bolivian Andes. It is not known what lies beneath it, but several potent brine springs (rich in NaCl) attest that halite must be present. The Locotal Breccia is overlain by rocks of the Limbo Formation, which include highly fractured beds of massive sandstone, *magnesite* and *dolomite*, containing some *talc* and *danburite* and commercially operated deposits of *magnesite*, *dolomite* and *magnesioriebeckitic asbestos* (e.g., San Francisco Mine near Villa Tunari, see Franz et al. 1979). The Limbo Formation, in part, may represent a slightly metamorphosed Cambrian "false marine carbonate caprock" like a similar but younger and unmetamorphosed rock in Mississippi (Swan - Saunders 1992). The youngest strata of the Limbo Formation are coarse conglomerates of Cambrian or early Ordovician age containing rounded boulders of schists, granitic rocks and a rare granitic pegmatite, presumably derived from rocks of the Precambrian Brazilian shield. These sediments are followed by the monotonous sedimentary Ordovician and Silurian series typical of much of the Bolivian Andes (Franz et al. 1979).

The Locotal Breccia is composed (in approximate descending order of abundance) of a fine-grained aggregate of *dolomite, magnesite, gypsum, anhydrite, K-feldspar, talc,* and *smectites.* Additional minerals occur in minor or accessory amount, some of them included in the groundmass as euhedral crystals (in alphabetic order): *boracite, chalcopyrite, clinopyroxene, danburite, dravite, ericaite, graphite, hematite, magnesioferrite?, minnesotaite?, polyhalite, povondraite, pyrite, rutile,* and *tennantite*. The metacrysts of some these minerals can reach the size up to several centimetres. The most common is *danburite*, which

is also the best known mineral from the Locotal Breccia. It occurs in many places in almost all outcrops of the Locotal Breccia. The crystals are double-terminated, in contrast to other famous world *danburite* localities and they can reach up to 6 cm in length. The crystals are grey and of greasy lustre; the coloration is caused by many tiny inclusions predominantly *dolomite*, *talc*, *anhydrite* and opaque phase, probably *pyrite*. *Boracite* is much rarer than *danburite*. Additional occurrences of *boracite* have been found during our recent field investigations and one place yielded large green crystals up to almost 3 cm, having the form of a simple cube. However, most abundant are tiny colourless crystals about 1 mm in size, showing a ball-like form. All *boracite* crystals display polycrystalline, very fine parquet-like structure under the polarizing microscope, in crossed polarizers. Among other minerals forming single euhedral, up to 2-3.5 cm sized metacrysts, *dolomite* and *magnesite* are most common, the former as black, black-brown, white or bluish rhombohedrons, the latter as platy, pseudohexagonal crystals, colourless or with yellowish coloration. *Hematite* forms loose platy crystals with typical triangular striation reaching a size of 15 x 12 x 5 mm. Recent solution cavities in the breccia are filled with secondary acicular *aragonite* or stalactitic *calcite* or *aragonite*. Other supergene minerals found in the breccia are *azurite, goethite, hydromagnesite, mcguinessite,* and *malachite*.

The evaporite breccia includes also angular cm-dm sized clasts ("xenoliths") of silicate-rich highly alkaline rocks in its groundmass. They reacted with the surrounding evaporite matrix to form crystal crusts composed of *potassium feldspar* (*microcline*), tourmalines (*povondraite* and *schorl-dravite*), *magnesioriebeckite, hematite*, and *pyrite*; less common are *rutile, clinopyroxene,* and *clinochlore*. Other "xenoliths", not associated with tourmalines, are represented by sandstone and monomineralic *quartz* and *lizardite* clasts, but they appear to have been non-reactive and have no crystal crusts (Petrov 1994, Petrov et al. 1997). The largest and best-shaped crystals of silicate minerals occur as components of crystal crusts on the surface of the "xenoliths", but they also occur in massive form as veinlets or directly in the matrix of the clasts. The most common mineral is *microcline* (determined by X-ray analysis) as pink, lenticular crystals composing druses. It displays a red luminescence in a short-wave UV-light. White tiny pseudohexagonal crystals were found growing on *povondraite* crystals. *Povondraite* commonly forms black, short prismatic crystals reaching about 5 mm, growing on two types of "xenoliths" (samples B-2, B-3, see further in the text), locally it also forms veinlets or metacrysts in these xenoliths. The crystals of *povondraite* are sometimes covered by younger crystals of poorly determined *clinopyroxene (diopside* or *aegirine)*, and yellowish *magnesite*. Besides *povondraite*, members of *schorl-dravite* series (closer to dravite) are common on a certain type of the xenoliths (sample B-1, see further in the text). In contrast to the short prismatic *povondraite*, this deep-brown to black tourmaline forms columns and needles up to 1 cm long, or radiating aggregates.

Samples and methods

Four typical silicate-rich "xenoliths" with tourmalines, newly sampled by two of the authors (A. P. and J. H.), were studied. Two slightly different rocks studied (B-2, B-3) are rich in macroscopic povondraite, one rock (B-1) is rich in coarse dravite and one sample (B-4) contains accessory tourmalines seen only under the microscope. Chemical compositions were determined using energy dispersive electron microprobe Camscan-Link-eXL with operating conditions of 20 kV, 3 nA, counting time 80s, and Co as calibration element. Synthetic oxides, plagioclase and K-feldspar were used as standards. Because of lack of sufficient material for wet analyses, chemical composition of the samples, was estimated by integrating scanning analyses covering area of 5 x 4 mm. The presence of Cr, Ti, Ba, V, Sr was verified in the wavelength-dispersive mode using a MICROSPEC spectrometer (Ba, V, Sr were analysed but not detected). The analyses were made in the laboratories of the Czech Geological Survey in Prague, I. Vavřín, analyst. The microprobe analyses obtained were recalculated using computer program MINCALC (Melín - Kunst 1992). Tourmaline compositions (including povondraite) were calculated on the basis 31 anions assuming stoichiometric amount of OH = 4 and B = 3 without the ordering of cations into crystallochemical sites (compare Grice - Ercit 1993). For povondraite, all Fe is assumed to be Fe^{3+}, because standard recalculation schemes lead to overestimate of Fe^{2+} (Grice - Ercit 1993, Grice et al. 1993). For dravite, all Fe is assumed to be Fe^{2+}, although some Fe^{3+} is most probably also present. Mica compositions were normalized based on 20 oxygen atoms and 4 OH groups, and assuming all Fe to be divalent.

Petrology and bulk compositions of "xenoliths" with tourmaline

The samples studied are represented by 2-4 cm long fragments of silicate-rich, but quartz-free rocks occurring as clasts or "xenoliths" in the Loccotal Breccia. All the rocks studied are composed besides tourmalines predominantly of K-feldspar and phlogopite with rutile and pyrite as minor to accessory phases. Minor aegirine was found in sample B-1. A comparison of chemical analyses of the rocks studied reveals significant differences between the rocks with povondraite and those with schorl-dravite (compare samples B-1 - B-4 in Table 1). There are relatively small differences in SiO_2 (42-50 wt.%) and Al_2O_3 (12.2-15.5 wt.%), all rocks are relatively rich in TiO_2 (0.85-3.00 wt.%) and poor in CaO (0.0X-0.34 wt.%). The rocks rich in povondraite have extremely high concentrations of K_2O (10-12 wt.%), low Na_2O (0.4-0.7 wt.%), very low CaO (0.0X-0.13 wt.%) and increased Cr_2O_3 (about 0.1 wt.%),

whereas the rock rich in schorl-dravite is slightly richer in CaO (0.34 wt.%) and the concentrations of both Na_2O and K_2O are about 4 wt.%. The concentrations of MgO (2.6-9.0 wt.%) and FeO^{tot} (5.4-13.0 wt.%) are variable and independent on given type of tourmaline.

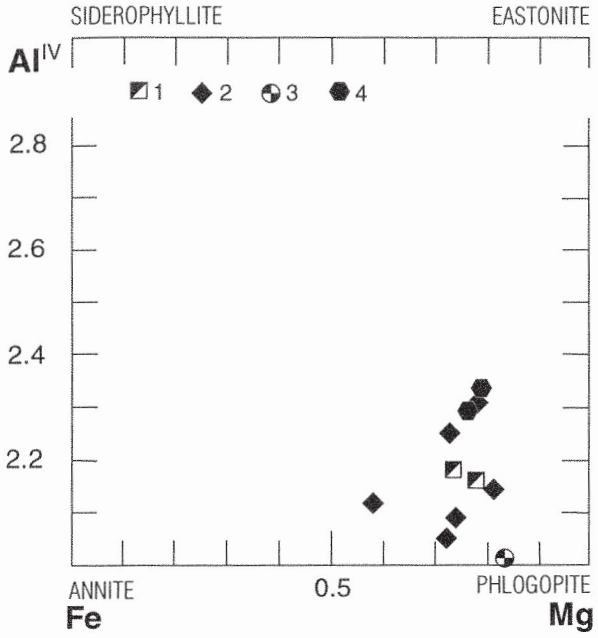

Fig. 1. Al^{IV}- Mg/(Mg + Fe^{tot}) diagram for mica from Locotal Breccia. Two mica compositions with Al^{IV} = 1.7-1.9 fall out of this diagram. Symbols 1-4 represent samples B-1-4

Sample B-1 is represented by apple-green to pale grey-green massive material with two parallel zones with the intensive blastesis of the black (at the edges brown) tourmaline, much coarser than the matrix. On the surface of the clast, tourmaline forms clusters of columnar to acicular crystals, 1-3 mm in size, together with minute crystals of K-feldspar.

Yellow-green fine matrix, rich in tiny inclusions prevails (about 60 vol.%), along with randomly dispersed colourless grains and crystals of K-feldspar (about. 10 mod.%), which frequently includes fine sagenitic brown rutile. Tourmaline (about 30 vol.%) forms euhedral grains 0.X-2 mm in size, composing several mm up to 1 cm sized aggregates. The crystals are optically zoned, with darker zone of the variable thickness near the edge. Wide centres display significant pleochroism (ε-very light brown, ω-deep olive green), the rims are still darker (ε-pale brown-yellow, ω-deep olive green). Pyrite is accessory. By electron microprobe, potassium feldspar was identified as the only colourless mineral. Dominant green matrix mineral is mica close to phlogopite with X_{Mg} = Mg/(Mg + Fe) = 0.74-0.78 and Al^{IV} = 2.16-2.19 (see Fig. 1). Taking into account the highly oxidic mineral assemblage, a portion of Fe could be present as Fe^{3+}. The concentrations both of TiO_2 and Na_2O in the mica are low (0.3-0.4 and 0.2 wt.%, respectively). Tourmaline is schorl-dravite (X_{Mg} = 0.71-0.83), for details see further in the text. Clinopyroxene close to the end-member aegirine was detected by microprobe as tiny inclusions (10-50 microns) concentrated mainly in centres in tourmaline crystals. The *aegirine* analysed has the following composition: SiO_2 = 53.5-54.9, Al_2O_3 = 1.0-1.4, $Fe_2O_3^{tot}$ = 28.5-31.0, MgO = 0.3-0.8, Na_2O = 12.9-13.3, all in wt.%. Increased bulk Na_2O concentrations (4.14 wt.%, see Table 1), imply the rock most probably contains many aegirine inclusions in the matrix. Rutile nearly corresponds to pure TiO_2, with only slightly increased concentration of FeO (about 1.3 wt.%).

Sample B-2 represents in hand-specimen massive grey-brown rock with isolated prismatic crystals of pink K-feldspar. Much smaller, lath-shaped to acicular crystals of K-feldspar occur as a component of the fine-grained matrix. Tourmaline (povondraite) occurs as black crusts and small crystals on the surface of the clast and as 0.X mm wide veinlets.

The rocks displays ophitic texture, dominated by lath-shaped to acicular crystals of potassium feldspar, which prevails over light-green or yellow-green, slightly pleochroic mica. Tourmaline occurs both as accumulations of anhedral grains and as well-shaped crystals concentrated in thin veinlets. In addition, small anhedral grains and aggregates of povondraite are disseminated in the matrix.

Table 1. The average of n scanning microprobe chemical analyses, each covering area 5 x 4 mm of four most common "xenoliths" in the Locotal Breccia. B-3, B-2 - the rocks with povondraite, B-1 - the rock with schorl dravite, B-4 - the rock poor in tourmaline but with three successive populations of accessory tourmaline

sample	B-3		B-2		B-1		B-4	
	n=3	average	n=3	average	n=3	average	n=2	average
SiO_2	48.40 - 49.27	48.87	49.15 - 49.92	49.58	39.94 - 43.42	41.50	45.34 - 46.47	45.91
TiO_2	2.96 - 3.03	3.00	1.54 - 2.02	1.84	0.72 - 0.95	0.85	1.29 - 0.36	1.32
Cr_2O_3	0.0 - 0.11	0.00	0.0 - 0.13	0.00	0.0	0.00	0.0 - 0.13	0.00
Al_2O_3	12.85 - 13.24	13.03	15.29 - 15.62	15.47	10.98 - 16.79	13.54	12.08 - 12.40	12.24
CaO	0.00	0.00	0.08 - 0.16	0.13	0.23 - 0.47	0.34	0.25 - 0.26	0.26
FeO_{tot}	11.17 - 12.33	11.87	5.09 - 5.72	5.39	12.60 - 13.75	13.00	7.82 - 7.95	7.89
MgO	2.47 - 2.81	2.64	8.86 - 9.04	8.96	7.74 - 8.78	8.17	8.68 - 8.79	8.73
MnO	0.0 - 0.09	0.00	0.00	0.00	0.0 - 0.10	0.00	0.0 - 0.14	0.00
K_2O	9.82 - 10.39	10.12	11.73 - 12.23	11.97	2.30 - 5.47	4.03	9.24 - 9.54	9.39
Na_2O	0.64 - 0.69	0.66	0.39 - 0.41	0.40	3.96 - 4.32	4.14	2.02 - 2.18	2.10
Tot	89.62 - 91.08	90.19	93.30 - 94.74	93.76	83.84 - 87.76	85.57	87.12 - 88.81	87.83

Tourmaline is strongly pleochroic with ε-light cinnamon brown, ω-deep brown-black. Rutile and pyrite are accessory. The composition of green mica is variable, (Fig. 1), corresponding to annite-phlogopite solid solution (XMg = 0.57-0.83, Al^{IV} = 1.70-2.14), with strongly variable concentrations of TiO_2 (0.2-3.8 wt.%) and Na_2O (0.1-1.1 wt.%). A deficiency of Al^{IV} (in two analyses Al^{IV} = 1.7 and 1.9) indicates significant replacement of Al by Fe^{3+} in tetrahedral sites. The povondraite is compositionally zoned, generally, with a rimward increase in Al (at the expense of Fe), and with many oscillations in composition, characterized in the following text. Besides povondraite, accessory dravite was found as 20 microns long inclusion in the matrix.

Sample B-3 is massive fine-grained rock in hand-specimen, with grain size near 1 mm, black and light yellowish speckled, resembling by its appearance serpentinite. It is composed mainly of K-feldspar and tourmaline (povondraite), the modal compositions of both minerals being mostly between 40-60 vol.%. Speckled light portions with a prevalence of potassium feldspar may pass continuously into massive black, cm-sized accumulations formed by nearly monomineralic povondraite. Povondraite also forms crystalline crusts and crystals on the surface of the clast.

Under the microscope, the rock is composed of an aggregate of randomly oriented, lath-shaped colourless crystals of K-feldspar and of grains and accumulations (mostly anhedral) of strongly pleochroic povondraite (pleochroism is the same as in sample B-2). Light yellow-green mica is present only as rare relics in tourmaline. It displays composition similar to phlogopite from samples discussed above (X_{Mg} = 0.84, Al^{IV} = 2.02, see Fig. 1). Textural criteria indicate that povodraite grew at the expense of phlogopite. Compositionally, the povondraite is richer in TiO_2 relative to sample B-2, however the zonation of crystals is indistinct. Hematite with increased concentration of TiO_2 (2.6 wt.%) and sagenitic rutile are accessory minerals.

Sample B-4 represents a massive fine-grained (grain size 0.X mm) grey-green couloured rock without bigger porphyroblasts, suggesting in the hand-specimen weathered greywacke or rather a chloritized volcanic tuff. Under the stereomicroscope, green and colourless grains are visible besides pyrite and rare crystals and crusts of black tourmaline (0.X mm) are sitting predominantly on the surface of the clast.

Under the polarizing microscope, the rock represents a uniform mosaic of tiny lath-shaped feldspars and of slightly pleochroic greenish mica compositionally close to phlogopite (X_{Mg} = 0.77, Al^{IV} = 2.3, TiO_2 = 0.2-0.3 wt.%, Fig. 1). K-feldspar strongly prevails but minor (or accessory) oligoclase, 19 An, was found by microprobe. Rare tourmaline (0.X vol.%) forms corroded columns (up to 0.5 x 0.4 mm in size), is pleochroic (ε-pale brown, nearly colourless, ω-cinnamon brown), but locally irregular pale-blue and deeper-brown spots appear in the centres. In addition, the tourmaline porphyroblasts include tiny irregular inclusions of deep-brown tourmaline 10-40 microns in size.

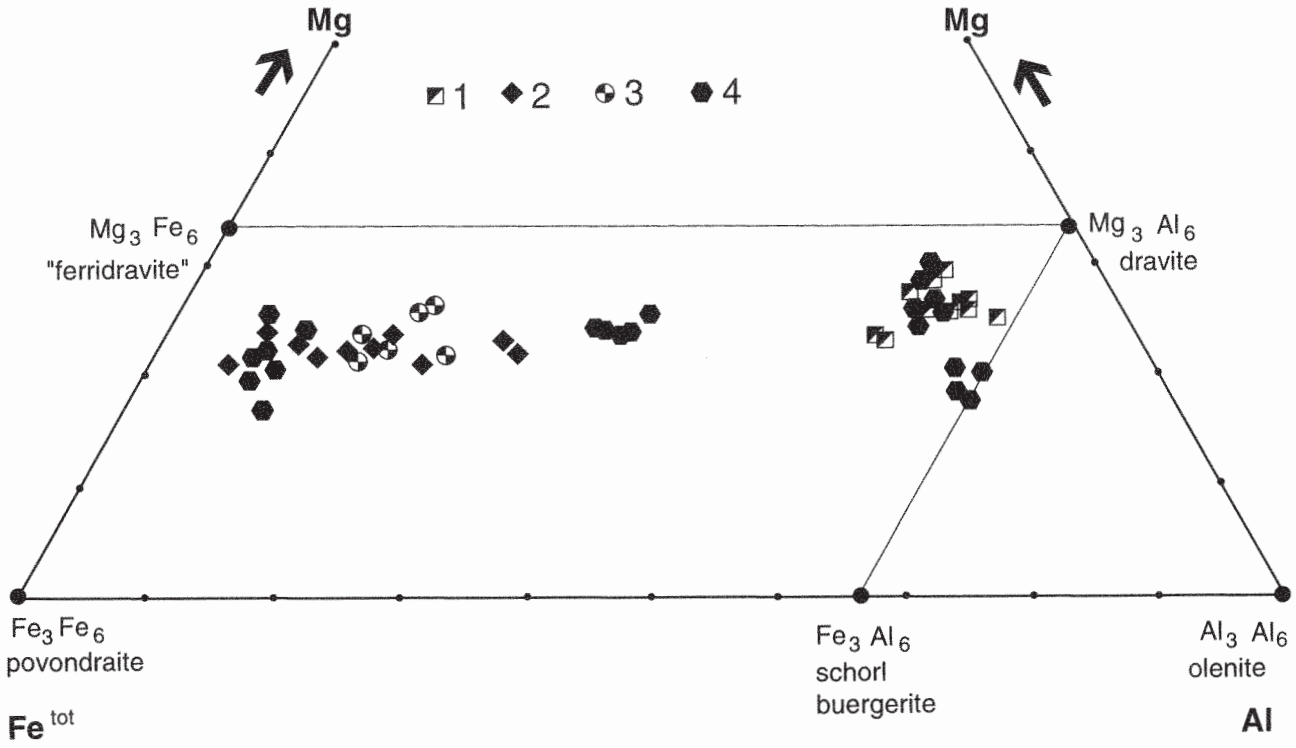

Fig. 2. Fe^{tot}-Al-Mg diagram for tourmaline from Locotal Breccia
Symbols 1-4 represent samples B-1 - B-4. Due to the incorporation of Mg into the Y-site and Z-site (see Grice et al. 1993), the povondraite compositions fall seemingly closer to the end-member $NaMg_3Fe_6^{3+}(BO_3)_3(Si_6O_{18})(O,OH)_4$, "ferridravite"

Chemical composition of tourmaline

Two different dominant tourmaline types occur as crystal crusts and also in the matrix of silicate clasts of various compositons included as "xenoliths" in the metaevaporite (Fig. 2). Povondraite occurs as stubby prisms and anhedral grains in matrix of ultrapotassic, low-Na, Ca-poor rocks, whereas tourmaline of the schorl-dravite series (columnar to acicular) grew in rock with K_2O and Na_2O concentrations about 4 wt.% and CaO about 0.3 wt.% (Table 1).

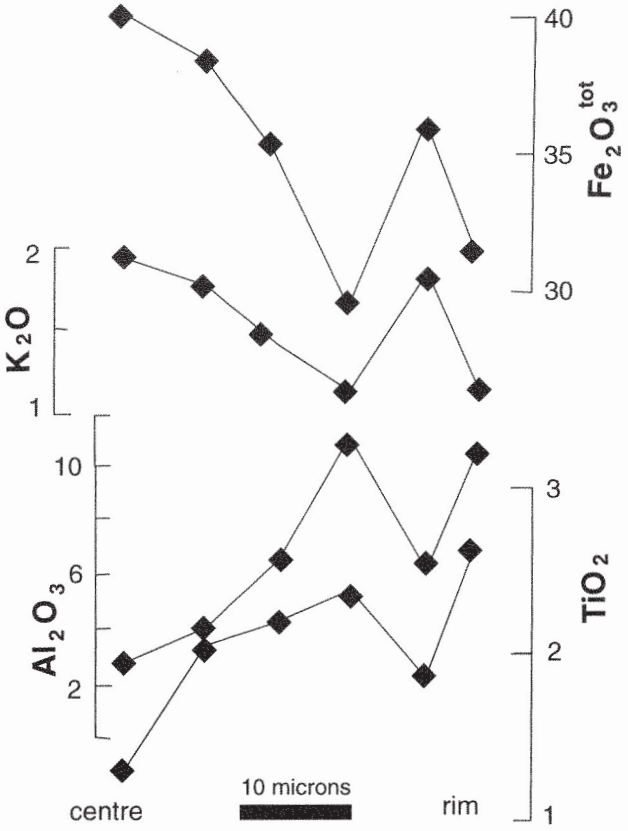

Fig. 3. Compositional profile in povondraite porphyroblast, sample B-2

Povondraite displays significant variations controlled by different chemical compositions of the parent-rock and by zoning in the range of the crystal. Euhedral povondraite from the sample B-2 displays pronounced growth zoning characterized by a rimward increase in Al and Ti and decreased Fe, K and K/(K + Na). However, a significant oscillation near the rim exhibits an opposite trend (Fig. 3, Table 2, analyses 3181-3184) which is different from that established by Grice et al. (1993). Potassic compositions with X_K = K/(K + Na) > 0.5 described by Grice et al. (1993) were not found, however compositions with X_K = 0.40-0.46 are quite frequent both in the centre of the crystals and near the edge (see Fig. 4). The concentrations of individual oxides vary in the range (wt.%): Al_2O_3 = 2.39 (wide centres) -10.90 (narrow marginal zone), TiO_2 = 0.38-2.65, Na_2O = 1.45-2.29, K_2O = 1.15-1.92; the concentrations of Cr_2O_3 and MnO are mostly lower than 0.1 wt.% (Fig. 2). Minor oscillatory zoning was observed in

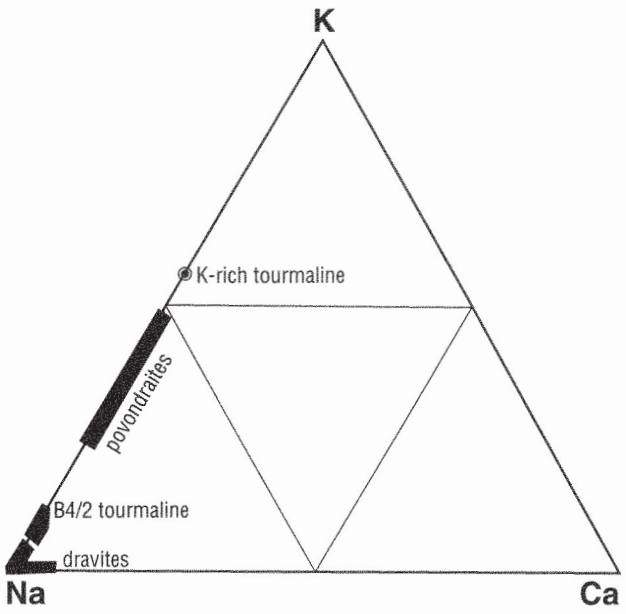

Fig. 4. Na-Ca-K diagram for tourmalines from Locotal Breccia. K-rich tourmaline composition from Grice et al. (1993). B4/2 tourmaline is intermediate povondraite-dravite from sample B-4

anhedral povondraite from the sample B-3. Generally, B-3 povondraite is more aluminous (Al_2O_3 = 5.15-8.78), with variable concentrations of TiO_2 = 1.46-3.48, Na_2O = 1.58-2.13 and K_2O = 1.28-2.35 and traces of Cr_2O_3 = 0.0X-0.26 (all in wt.%, see Table 2, Fig. 2).

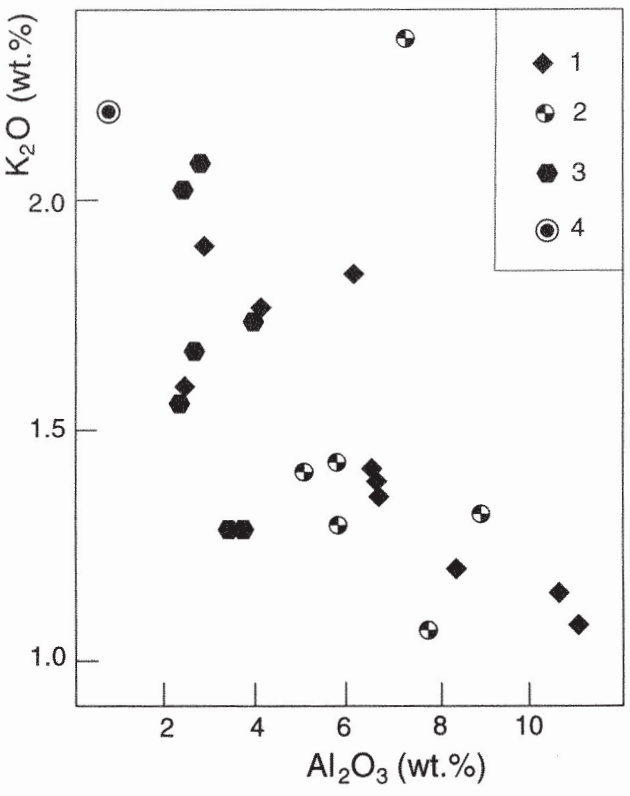

Fig. 5. K_2O-Al_2O_3 diagram for povondraite from Locotal Breccia
1 - sample B-2; *2* - sample B-3; *3* - sample B-4; *4* - K-rich tourmaline from Grice et al. (1993)

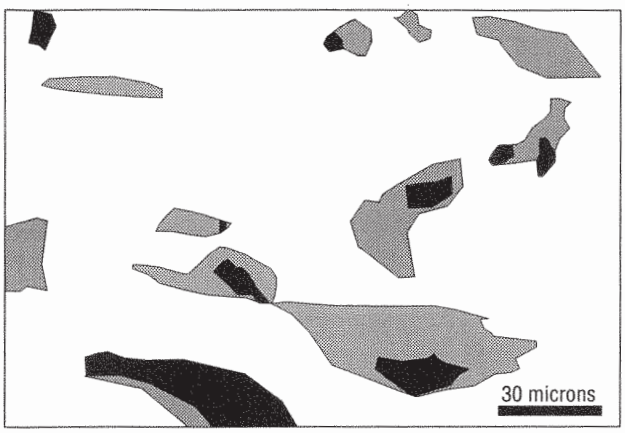

Fig. 6. Line-draving based on back-scattered electron image of tourmaline from sample B-4
Black - povondraite (TUR-1); *gray* - intermediate povondraite-dravite (TUR-2); *white* - schorl-dravite (TUR-3)

Tourmaline from sample B-1 is schorl-dravite with prevalence of the dravite component (Fig 2). The values of Mg/(Mg + Fe) range from 0.63 to 0.73 considering all Fe as FeO^{tot}. The tourmaline displays minor zonation with rimward increase in TiO_2 (0.0-0.49) and FeO^{tot} (7.7-10), compensated by a decrease in Al_2O_3 (30.1-25.9), all in wt.%, but many oscillations appear (see Table 3). The tourmaline contains a slightly variable concentration of MgO = 9.2-10.4 wt.%, low CaO (0.0X-0.34 wt.%), with negligible MnO and Cr_2O_3. The X-site occupancy is close to 1.

Tourmaline of similar composition was found in the matrix of sample B-2 as rare, isolated inclusions, several tens of microns in diameter, without any relation to associated povondraite (Table 3). It contains a higher concentration of TiO_2 = 1.6-1.7 wt.%, and is poorer in CaO (lower than 0.1 wt.%) compared to the sample B-1.

Sample B-4 displays a highly unusual tourmaline assemblage. It contains tourmaline as a rare accessory but three successive tourmaline populations were distinguished (Fig. 2). The dominant tourmaline is schorl dravite (TUR-3), compositionally close to B-1 tourmaline. It includes tiny anhedral inclusions of povodraite (10-40 microns in size) and inclusions of unusual tourmaline of intermediate povondraite-dravite (schorl) composition (10-100 microns in size, Tab. 4). All three tourmalines are well recognizable in electron backscattered image (Fig. 6). Textural criteria indicate that the oldest tourmaline-povondraite (TUR-1), is overgrown and partly replaced by younger TUR-2 tourmaline. The povondraite is rich in TiO_2 = 0.79-3.44 wt.%, equal to 0.12-0.39 apfu, and displays increased but very variable Cr_2O_3 concentrations (0.0-1.36 wt.%, equal 0.0-0.21 apfu). However, Al_2O_3 (2.7-2.9 wt.%) and $Fe_2O_3^{tot}$ (38.4-40.5 wt.%) concentrations show remarkable uniformity compared to povondraites from samples B-2 and B-3. The unusual B4/2 tourmaline (TUR-2) is intermediate Ti-bearing povondraite-(schorl)-dravite, containing 3.3-3.6 TiO_2 (equal to 0.46-0.51 apfu), 0.0-0.6 Cr_2O_3 (equal to 0.00-0.09 apfu), 14-14.8 Al_2O_3, 23-24 $Fe_2O_3^{tot}$, 7.4-7.8 MgO, 2.6-2.8 Na_2O about 0.3 K_2O and low MnO and CaO (0.0X-0.2), all in wt.%.

Table 2. Electron microprobe analyses of povondraite. Analyses No 3181-3184 are representative from the compositional profile of sample B-2

sample	B-3	B-3	B-3	B-3	B-2	B-2	B-2	B-2	B-2
anal. N°	3157	3159	3161	3162	3174	3181c	3182	3183	3184r
SiO_2	31.96	32.66	33.11	32.12	31.06	32.17	32.13	32.41	33.22
TiO_2	2.31	1.46	2.05	3.48	0.38	1.26	2.04	2.20	2.34
Al_2O_3	5.71	7.71	7.19	5.15	2.39	2.93	4.11	6.57	10.91
Fe_2O_3	35.60	32.46	32.31	36.08	42.37	40.19	38.57	35.21	29.56
MnO	-	-	0.11	-	-	-	0.09	0.10	-
MgO	6.65	7.95	7.70	6.24	6.19	7.02	6.72	6.72	6.75
CaO	-	-	-	-	-	0.05	-	-	-
Na_2O	1.64	2.13	1.66	1.58	1.55	1.48	1.61	1.82	2.02
K_2O	1.44	1.07	2.35	1.41	1.60	1.92	1.77	1.39	1.09
$B_2O_{3\ calc}$	8.63	8.78	8.83	8.69	8.39	8.62	8.68	8.77	8.97
H_2O_{calc}	3.18	3.24	3.26	3.21	3.10	3.18	3.20	3.24	3.31
Total	97.13	97.45	98.57	97.95	97.03	98.82	98.91	98.42	98.17
Si	6.018	6.044	6.092	6.006	6.015	6.066	6.013	6.004	6.014
Al	1.268	1.681	1.558	1.135	0.546	0.650	0.906	1.434	2.328
Fe^{3+}	5.045	4.521	4.473	5.076	6.175	5.701	5.433	4.909	4.027
Ti	0.327	0.203	0.284	0.489	0.055	0.179	0.287	0.307	0.318
Mn	-	-	0.017	-	-	-	0.014	0.016	-
Mg	1.868	2.194	2.112	1.738	1.788	1.973	1.875	1.856	1.822
Ca	-	-	-	-	-	0.010	-	-	-
Na	0.600	0.764	0.592	0.573	0.583	0.540	0.583	0.653	0.710
K	0.347	0.253	0.551	0.336	0.396	0.461	0.424	0.329	0.251
B	3.000	3.000	3.000	3.000	3.000	3.000	3.000	3.000	3.000
O	27.000	27.000	27.000	27.000	27.000	27.000	27.000	27.000	27.000
OH	4.000	4.000	4.000	4.000	4.000	4.000	4.000	4.000	4.000

0.0X < Cr_2O_3 < 0.26 wt.%

Table 3. Electron microprobe analyses of tourmaline of schorl-dravite series. Analyses No 3205-3213 represent compositional profile from centre to rim

sample	B-2	B-2	B-1	B-1	B-1	B-1	B-1	B-1	B-1	B-1
anal. N°	3198	3202	3205c	3206	3207	3208	3209	3210	3211	3213r
SiO_2	36.46	36.63	37.35	37.11	37.20	37.32	37.58	37.19	36.78	36.37
TiO_2	1.67	1.71	0.12	-	0.08	0.25	0.22	0.69	0.49	0.49
Al_2O_3	24.58	24.49	28.15	28.16	28.49	27.72	30.17	25.92	26.13	26.32
FeO_{tot}	12.18	12.10	7.98	8.00	7.69	8.89	6.21	8.68	8.25	9.77
MnO	-	-	0.08	-	-	-	-	-	-	-
MgO	7.85	7.93	9.37	9.38	9.39	9.24	9.22	10.23	10.40	9.26
CaO	-	0.08	0.34	0.27	0.32	0.28	0.14	0.07	0.34	-
Na_2O	3.05	2.97	2.91	3.07	3.03	2.92	3.05	3.23	3.11	3.02
K_2O	0.09	0.20	-	-	-	-	-	-	-	0.06
$B_2O_{3\ calc}$	9.54	9.56	9.85	9.81	9.85	9.84	10.00	9.74	9.70	9.61
H_2O_{calc}	3.52	3.53	3.64	3.62	3.64	3.63	3.69	3.60	3.58	3.55
Total	98.94	99.20	99.78	99.42	99.68	100.08	100.28	99.34	98.77	98.45
Si	6.212	6.225	6.161	6.146	6.134	6.163	6.103	6.201	6.161	6.148
Al	4.936	4.905	5.473	5.497	5.537	5.395	5.775	5.093	5.158	5.243
Ti	0.214	0.218	0.015	-	0.010	0.031	0.026	0.086	0.062	0.063
Fe^{2+}	1.736	1.720	1.100	1.107	1.060	1.228	0.843	1.210	1.155	1.380
Mn	-	-	0.011	-	-	-	-	-	-	-
Mg	1.994	2.010	2.303	2.315	2.307	2.274	2.232	2.543	2.596	2.334
Ca	0.000	0.015	0.060	0.048	0.056	0.050	0.025	0.013	0.060	-
Na	1.008	0.979	0.930	0.985	0.968	0.936	0.959	1.044	1.011	0.989
K	0.020	0.044	-	-	-	-	-	-	-	0.013
B	3.000	3.000	3.000	3.000	3.000	3.000	3.000	3.000	3.000	3.000
O	27.000	27.000	27.000	27.000	27.000	27.000	27.000	27.000	27.000	27.000
OH	4.000	4.000	4.000	4.000	4.000	4.000	4.000	4.000	4.000	4.000
X_{Mg}	0.535	0.539	0.677	0.676	0.685	0.649	0.726	0.678	0.962	0.628

$0.0X < Cr_2O_3 < 0.17$ wt.%

Table 4. Electron microprobe analyses of three successive tourmaline populations, sample B-4 (TUR 1-3, see Fig. 6)

B-4	TUR 1	TUR 1	TUR 1	TUR 1	TUR 2	TUR 2	TUR 2	TUR 3	TUR 3	TUR 3
anal. N°	3677	3671	3672	3681	3673	3674	3683	3676	3686	3687
SiO_2	31.46	31.78	31.10	30.24	33.79	33.64	34.18	36.29	36.61	37.03
TiO_2	0.79	1.15	2.66	3.44	3.60	3.32	3.56	0.22	0.17	0.51
Cr_2O_3	-	0.65	1.36	0.74	0.24	0.61	-	0.08	0.10	0.10
Al_2O_3	2.90	2.62	2.71	2.76	13.96	14.03	14.82	26.90	29.56	26.64
Fe_2O_3	40.52	38.53	38.83	36.91	23.81	24.05	22.99	-	-	-
FeO	-	-	-	-	-	-	-	8.52	9.96	8.33
MnO	-	0.09	-	0.15	-	-	0.19	-	-	-
MgO	6.36	7.87	5.62	5.85	7.38	7.44	7.77	9.33	6.86	9.71
CaO	0.24	-	-	-	-	-	0.07	0.10	0.16	-
Na_2O	1.47	1.98	1.81	1.62	2.73	2.60	2.81	3.02	2.91	3.03
K_2O	2.12	1.55	1.65	2.06	0.31	0.31	0.27	0.28	-	-
$B_2O_{3\ calc}$	8.45	8.50	8.36	8.22	9.18	9.15	9.32	9.60	9.77	9.70
H_2O_{calc}	3.12	3.14	3.08	3.03	3.39	3.38	3.44	3.54	3.61	3.58
Total	97.43	97.86	97.18	95.02	98.39	98.53	99.42	97.88	99.71	98.63
Si	6.046	6.077	6.047	5.978	5.982	5.971	5.957	6.144	6.090	6.201
Al	0.657	0.590	0.621	0.643	2.913	2.939	3.044	5.367	5.795	5.258
Fe^{3+}	5.860	5.544	5.681	5.491	3.172	3.212	3.015	-	-	-
Cr	-	0.099	0.209	0.115	0.033	0.086	-	0.011	0.013	0.013
Ti	0.117	0.165	0.389	0.511	0.479	0.443	0.467	0.028	0.021	0.064
Fe^{2+}	-	-	-	-	-	-	-	1.206	1.386	1.167
Mn	-	0.015	-	0.025	-	-	0.028	-	-	-
Mg	1.822	2.243	1.629	1.724	1.948	1.969	2.019	2.355	1.701	2.424
Ca	0.050	-	-	-	-	-	0.013	0.018	0.029	-
Na	0.548	0.734	0.682	0.621	0.937	0.895	0.950	0.992	0.939	0.984
K	0.520	0.378	0.409	0.520	0.070	0.070	0.060	0.060	-	-
B	3.000	3.000	3.000	3.000	3.000	3.000	3.000	3.000	3.000	3.000
O	27.000	27.000	27.000	27.000	27.000	27.000	27.000	27.000	27.000	27.000
OH	4.000	4.000	4.000	4.000	4.000	4.000	4.000	4.000	4.000	4.000
X_{Mg}								0.661	0.551	0.675

Discussion

This paper presents new compositional data on an unusual tourmaline assemblage including povondraite (22 analyses, Figs. 2-5, Tables 2, 4), intermediate Ti-bearing povondraite-dravite (5 analyses, Fig. 2, Table 4) and schorl-dravite (20 analyses, Fig. 2, Tables 3, 4), along with compositional data on mica close to phlogopite (Fig. 1) and aegirine (in the text). Four samples with tourmalines (povondraite and schorl-dravite) occurring as "xenoliths" in metaevaporite are characterized by bulk chemistry (Table 1).

Povondraite occurs in ultrapotassic Na-low, Ca-poor rocks (SiO_2 = 48-50 wt.%, K_2O = 10-12 wt.%, Na_2O = 0.4-0.7 wt.%, CaO = 0.0X-0.13 wt.%), whereas tourmaline of the schorl-dravite series grew in rock with SiO_2 concentration about 42 wt.%, K_2O and Na_2O concentrations about 4 wt.% and the CaO concentration about 0.3 wt.% (Table 1). Although the chemical composition and mineral assemblage of "xenoliths" are probably influenced by metasomatism, high concentrations of alkalis and the presence of relic aegirine indicate that these rocks originally represented highly alkaline volcanites close to phonolite.

No simple equation modelling the formation of tourmaline can be put together but the textural criteria indicate, that tourmalines studied grew predominantly at the expense of mica compositionally close to phlogopite, and in some cases also aegirine (sample B-1). Boron was evidently supplied by fluid from evaporite. The main factor favouring growth of either povondraite or tourmaline of schorl-dravite series seems to be bulk composition, mainly the concentration of alkalis and CaO, while the presence and concentrations of other major oxides played only a minor role (see Table 1). One of the rocks with povondraite studied (B-3) is rich in accessory hematite and pyrite but other rocks (including those with schorl-dravite) contain only pyrite.

All povondraite analyses are characterized by a very low CaO concentration (mostly bellow the detection limit) and a stable concentration of MgO ranging from 6 to 8 wt.%. The K/(K + Na) values vary between 0.25-0.48, the X-site occupancy is close to 1 (Fig. 4). Significant negative correlation between K_2O and Al_2O_3 (Fig. 5), shows that the compositions with lowermost Al_2O_3, nearest to the ideal formula of povondraite, $NaFe_3^{3+}Fe_6^{3+}(BO_3)_3(Si_6O_{18})(O,OH)_4$, contain the highest K_2O concentration (corresponding up to 48 % K in X-site) and tend therefore towards a potential new tourmaline species "K-povondraite" (see also Grice et al. 1993). The povondraites newly analysed are also significantly richer in TiO_2 (0.38-3.48 wt.% equal to Ti = 0.06-0.45 apfu), in contrast to Ti-poor povondraite compositions (with $TiO_2 < 0.1$ wt.%) given both by Walenta - Dunn (1979) and Grice et al. (1993). The highest TiO_2 and K_2O concentrations recorded (3.48 and 2.35 wt.%, respectively) represent the upper concentration levels of these oxides in tourmaline (Henry - Dutrow 1996), with one exception of TiO_2 concentration up to 4.07 wt.% (Lottermoser - Plimer 1987). Successive crystallization of three populations of tourmaline (sample B-4) with decrease Fe_{tot} and Fe^{3+} reflects probably the changes in fluid composition and mainly a decreasing of oxygen activity during crystallization (Table 4, Fig. 6).

From geological viewpoint, the probable sequence of events is as follows: A dieply buried saltdome (Cambrian or Upper Proterozoic) was intruded by dikes of highly alkaline rock(s), probably close to phonolite and affected by volcanite-derived fluids. Brittle deformation of the dikes started by diapiric movement of the salt. Evaporite-derived boron and other elements in the fluids reacted with the brecciating volcanites to form the povondraite, schorl-dravite, and other minerals. Evidence that reaction continued during successive stages of brecciation is provided by the fact that different faces of single angular volcanite clast often show tourmaline crusts of varying crystal size and type. Complex brecciation occurs in the caprock over a long period of constant diapiric uplift. After the Andean orogeny, uplift and erosion exposed the caprock on the surface in a tropical rainforest, where halite was leached and anhydrite was converted to gypsum. Present leaching of halite and gypsum continues at ambient temperature, further concentrating the carbonates and silicates in eluvia.

Few occurrences of tourmalines in metaevaporite rocks are reported in the literature. In general, the tourmaline associated with anhydrite and halite is dravite, but little is currently known of their exact composition (see Henry - Dutrow 1996, Popov - Sadykhov 1962). A somewhat similar assemblage as in Alto Chapere was described by Cabella et al. (1987) from lower Permian Brianconnais sequence, Maritime Alps. Danburite mineralization with tourmaline in dolomitic beds in metapelites of probably lacustrine environment likely originated during diagenesis of evaporitic sediments and later recrystallized during Alpine metamorphism (probably favoured by volcanic activity). The danburite-bearing beds reach a thickness of several decimetres to about 5 metres, passing continuously into pelitic beds composed of fine-grained black dravite, graphite, quartz and minor phlogopite. Tourmaline contains 27-30 wt.% Al_2O_3, 6.4-11 wt.% MgO, 3.5-7.7 wt.% FeO^{tot} and up to 0.40 wt.% K_2O. At higher metamorphic grades, tourmaline takes on the unusual bulk composition of the original evaporite (Henry - Dutrow 1996). For example, a Mn-rich metaevaporite contains manganian dravite (Ayuso - Brown 1984). The high-pressure dravite-bearing Mg-rich schist from the Dora Maira Massif, western Alps, is considered to have originated as siliceous mudstone in an evaporitic environment (Schreyer 1977).

Acknowledgements. Authors are grateful to Dr. I. Vavřín for microprobe analyses and Dr. S. Vrána and Dr. M. Novák for criticism and instructive comments on the manuscript.

Submitted December 1, 1997

References

Ayuso, R. A - Brown, C. E. (1984): Manganese-rich red tourmaline from the Fowler talc belt, New York. - Canad. Mineral., 22, 327-332.

Cabella, R. - Cortosogno, L. - Lucchetti, G. (1987): Danburite-bearing mineralizations in metapelites of Permian age (Ligurian, Brianconnais, Maritime Alps, Italy). - Neu. Jb. Mineral., Mh., 289-294. Stuttgart.

Franz, E. D. - Ponce, J. - Wetzenstein, W. (1979): Geochemie und Petrographie der Magnesitlagerstttten des Alto Chapare/Bolivien. - Radex-Rdsch., 4, 1105-1119. Austria.

Grice, J. D. - Ercit, T. S. (1993): Ordering of Fe and Mg in the tourmaline crystal structure: The correct formula. - Neu. Jb. Mineral., Mh., 165, 3, 245-166. Stuttgart.

Grice, J. D - Ercit, T. S. - Hawthorne, F. C. (1993): Povondraite, a redefinition of the tourmaline ferridravite. - Amer. Mineralogist, 78, 433-436. Washington.

Henry, D. J. - Dutrow, B. L. (1996): Metamorphic tourmaline and its petrologic applications: *In: E. S. Grew - L. M. Anowitz* (eds.): Boron, mineralogy, petrology and geochemistry. - Rew. in Mineral., 33, 503-557, Mineral. Soc. Amer.

Lottermoser, B. G. - Plimer, I. R. (1987): Chemical variations in tourmalines, Umberatana, South Austalia. - Neu. Jb. Mineral. Mh., 314-326. Stuttgart.

Melín, M. - Kunst, M. (1992): MINCALC Development Kit. - MS Geol. úst. Akad. věd ČR. Praha.

Petrov, A. (1994): Aktuell: Der Neue Turmalin aus dem tropischen Regenwald Boliviens. - Extra Lapis 6 (Turmalin), 50-53.

Petrov, A. - Hyršl, J. - Žáček, V. (1997): The povondraite occurrence in Alto Chapare, Cochabamba, Bolivia. - Abstr., Tourmaline 1997 - Inter. Symp. on Tourmaline, June 20-25th, 68-69. Nové Město na Moravě.

Popov, V. S. - Sadykhov, T. S. (1962): Authigenic tourmaline from the Khodzha-Mumyn salt deposit. - Dokl. Akad. Nauk. SSSR, 145, 140-141. Moskva.

Schreyer, W. (1997): Whiteschists: their compositions and pressure-temperature regimes based od experimental, field, and petrographic evidence. - Tectonophysics, 43, 127-144. Amsterdam.

Swan, C. T. - Saunders, J. A. (1992): Cap rock geology of the Hazlehurst Salt Dome, Copiah County, Mississippi. - Gulf coast Assoc. of Geol. Societies, Transactions, 42, 697-705.

Walenta, K. - Dunn, P. J. (1977): Ferridravite, a new mineral of the tourmaline group from Bolivia. - Amer. Mineralogist, 64, 945-948. Washington.

Chemismus a původ hornin s povondraitem z Alto Chapare, Cochabamba, Bolívie

Povondrait a skoryl-dravit se vyskytují v metaevaporitu zvaném Locotal Breccia, patrně kambrického stáří, v Alto Chapare, provincie Cochabamba v centrálních bolívijských Andách. Turmalín společně s řadou silikátových minerálů vznikl pravděpodobně jako reakční krusty mezi žilnými intruzemi alkalických hornin a bórem bohatým evaporitem. Rozhodující roli při vzniku určitého typu turmalínu mělo chemické složení protolitu (hlavně různé koncentrace alkálií) a lokální aktivita kyslíku. Poměrně malé rozdíly jsou v koncentracích SiO_2 (42-50 hm.%) a Al_2O_3 (12,2-15,5 hm.%), všechny horniny jsou relativně bohaté TiO_2 (0,85-3,00 hm.%) a chudé CaO (0,0X-0,34 hm.%). Horniny bohaté povondraitem vykazují extrémně vysoké koncentrace K_2O (10-12 hm.%), málo Na_2O (0,4-0,7 hm.%) a jsou velmi chudé CaO (0,0X-0,13 hm.%). Naproti tomu horniny s turmalínem skoryl-dravitového typu jsou poněkod bohatší CaO (0,34 hm.%) a koncentrace Na_2O a K_2O se pohybují kolem 4 hm.%. Koncentrace MgO (2,6-9,0 wt.%) a FeO^{tot} (5,4-13,0 wt.%) silně kolísají u všech studovaných vzorků bez zjevné závislosti na daném typu turmalínu.

Krystaly povondraitu vykazují jak kontinuální, tak oscilační zonálnost a chemickou variabilitu kolísající v rozmezí (hm.%): $Fe_2O_3^{tot}$ = 29,5-42,4, Al_2O_3 = 2,39-10,90, TiO_2 = 0,38-3,48, Na_2O = 1,45-2,29, K_2O = 1,15-2,35, a silně kolísající Cr_2O_3 (0,0-1,36). Zjištěná chemická složení povondraitu se dosti výrazně liší od ideálního vzorce $NaFe_3^{3+}Fe_6^{3+}(BO_3)_3(Si_6O_{18})$ $(O,OH)_4$ zejména stabilní přítomností MgO v rozmezí 6-8 hm.% a přítomností draslíku v pozici X odpovídající 25-48 at.%. Povondrait s koncentrací TiO_2 nad 2,1 hm.% (>10 % v pozici Y) odpovídá podle Henry - Dutrow (1996) Ti-povondraitu (Ti-bearing povondraite). Nejvyšší analyzované koncentrace TiO_2 a K_2O (3,48 a 2,35 hm.%) představují vrchní koncentrační limity těchto oxidů zjištěné v turmalínu. Postupná krystalizace povondraitu (1), středního povondraitu-dravitu (2) a dravitu-skorylu svědčí pro pokles aktivity kyslíku během krystalizace turmalínu.